A Photocathode RF Gun Design for a mm-Wave Linac-Based FEL*

A. Nassiri, T. Berenc[†], J. Foster[†], G. Waldschmidt[†], and J. Zhou
Advanced Photon Source, Argonne National Laboratory
9700 South Cass Avenue, Argonne, Illinois 60439 USA

RECEIVED
JUN 19 1995
OSTI

Abstract

In recent years, advances in the rf gun technoloy have made it possible to produce small beam emittances suitable for short period microundulators which take advantage of the low emittance beam to reduce the wavelength of FELs. At the Advanced Photon Source, we are studying the design of a compact 50-MeV superconducting mm-wave linac-based FEL for the production of short wavelengths (~ 300 nm) to carry out FEL demonstration experiments. The electron source considered for the linac is a 30- GHz, 3 1/2-cell π–mode photocathode rf gun. For cold model rf measurements a 15-GHz prototype structure was fabricated. Here we report on the design, numerical modelling and the initial cold-model rf measurement results on the 15-GHz prototype structure.

I. INTRODUCTION

Short wavelength FELs impose stringent requirements on the quality of the electron beams. The key factor in obtaining a single-pass UV or x-ray FEL is the generation of small emittance elcetron beams with ultra-high brightness. In the past decade, a termendous amount of R&D has taken place to improve the performance of rf gun design [1-2]. With the emergence of new photocathode materials with good quantum efficiencies and improvements in laser technology to produce ultra-short pulses, it is now possible to produce small emittance electron beams suitable for short wavelength FEL applications. The linac structure being considered is a 60-GHz constant gradient superconducting stucture fabricated by using a precision microfabrication process known LIGA (Lithographie, Galvanoformung, Abformung).

The limitations on the emittance and beam brightness of an electron gun are mainly due to nonlinear electomagnetic forces, space charge forces, and the maximum current density that can be obtained from the cathode. Alkali semiconductors photocathode such as Cs_3Sb can produce peak current density of 600 A/cm^2. These cathodes may be operated at pulse lengths ranging from a few picoseconds to microseconds at high pulse repitition rates. However, excellent vacuum (~10^{-9} Torr) must be maintained. Field emission array (FEA) cathodes could produce current density in excess of 100 A/cm^2. However, at the present time, their limited liftime due to various breakdown modes does not make them attractive for accelerator applications.

II. RF GUN DESIGN

The rf gun considered for this project is a 30-GHz 3 1/2-cell structure. However, for ease of the initial fabrication and assembly, a prototype 15-GHz structure was designed and built as a first test structure. Although there are many technical difficulties associated with high-frequency rf gun structures, a 30-GHz photocathode rf gun allows us to reach very high gradient in excess of 500 MV/m. This drastically reduce the effects of space-charge forces and allows high-brightness beams. For a cylindrically symmetrical structure, the transvrse magnetic field (TM modes) can be unniquely determined by the axial electric field, E$_z$ [3]:

$$E_z(z, r) = E_z(z, 0) - \frac{r^2}{4}h(z) + O\left((pr)^4\right), \qquad (1)$$

$$E_r(z, r) = -\frac{r}{2}\frac{d}{dz}E_z(z, 0) - \frac{r^3}{16}h'(z) + O\left((pr)^5\right), \qquad (2)$$

$$B_\varphi(z, r)) = \frac{pr}{2c}E_z(z, 0) - \frac{pr^3}{16c}h(z) + O\left((pr)^5\right), \qquad (3)$$

where h(z) satisfies

$$h(z) = \left(\frac{d^2}{dz^2} + p^2\right)E_z(z, o) . \qquad (4)$$

For ideal cavity shape it is required to make both h(z) and h'(z) zero. In this case, the cavity's radius is given by [4]

$$r = \sqrt{\left(a^2 - \left(\frac{4d}{\pi}\right)^2\log\left(\sin\frac{\pi z}{2d}\right)\right)} \qquad (5)$$

As z goes to zero, it requires that r approaches infinity. In a real situation one can optimize the cells' geometry and the shape of the cavity around the exit in a way which is close to the ideal shape. The effects of nonlinear rf forces and self-fields of the electrons on the emittance growth of the electron beam has been described in detail by K.-J. Kim [5]. Emittance growth due to nonlinear rf forces can be controlled by ensuring that nonlinear transverse components of the rf fields are minimized. This can be achieved by placing a thick disk between cells and adjusting the diameter of the apertures so as to minimize nonlinear transverse components.The effects of nonlinear space charge forces are reduced since the initial electron distribution from the cathode are launched in a high gradient electric field and the space charge beam blowup scales as the inverse of the peak electric field gradient. For simulations, a laser pulse of 2 ps is chosen. MAFIA [6] numerical codes were used to

DISCLAIMER

DISCLAIMER

Portions of this document may be illegible
in electronic image products. Images are
produced from the best available original
document.

model the 3 1/2-cell rf gun including particle-in-cell simulations. The main parameters of the prototype photocathode rf gun are listed in Table 1.

Table 1: 15 GHz Prototype Gun RF Parametters

Parameter	Value
Frequency	15 GHz
Peak accelerating gradient	200 MV/m
Exit beam energy	4 MeV
Charge per bunch	1 nC
Cathode radius	0.5 mm
Emittance	2 mm-mrad
Shunt impedance	254 MΩ/meter
Q	7000

The gun's cell radius and aperture diameter were optimized to provide the correct longitudinal aceelerating field for the desired π-mode. For particle-in-cell simulations, a Gaussian bunch of 2-ps length (FWHM) and a total number of particles of 6×10^9 (total charge/bunch = 1 nC) is assumed to be ejected from the copper cathode surface of radius 0.5 mm. The initial velocity of the bunch is assumed to be v= 0.01 c with a peak rf accelerating gradient of 200 MV/m. Figure 1 shows the longitudinal field pattern for the accelerated bunched beam. Figure 2 is a plot of the particles energy (γ–distribution) along the z-axis.

III. PROTOTYPE GUN RF MEASUREMENTS

The field perturbation method was employed to determine the axial field distributions of the excited modes in the 15-GHz prototype rf gun structure. The perturbation is achieved by using small cylindrical aluminum beads deposited on nylon lines and optical fibers with a diameter of ~100 μm. A stepping motor with a 0.1-μm minimum step size was used to pull the bead through the structure. For a bead having dimension that is small compared to the structure wavelength, the perturbation relation is given by [7]

$$\frac{\Delta f}{f_0} \approx \frac{3\Delta V}{4U}\left[\varepsilon_o\left(F_1|E_{\parallel}|^2 + F_2|E_{\perp}|^2\right) - \frac{\mu_o}{2}\left(F_3|H_{\parallel}|^2 + F_4|H_{\perp}|^2\right)\right]$$

(6)

where $E_{\parallel}$ ($E_{\perp}$) and $H_{\parallel}$ ($H_{\perp}$) are the electric and magnetic fields parallel (perpendicular) to the perturbing object axis and F_n (n=1,2,3,4) are the perturbational form factors. For a metallic sphere, these form factors are all equal to 1 [6].

The measurement setup (Figure 3) consists of two shorting plates located at the entrance and the exit of the structure to

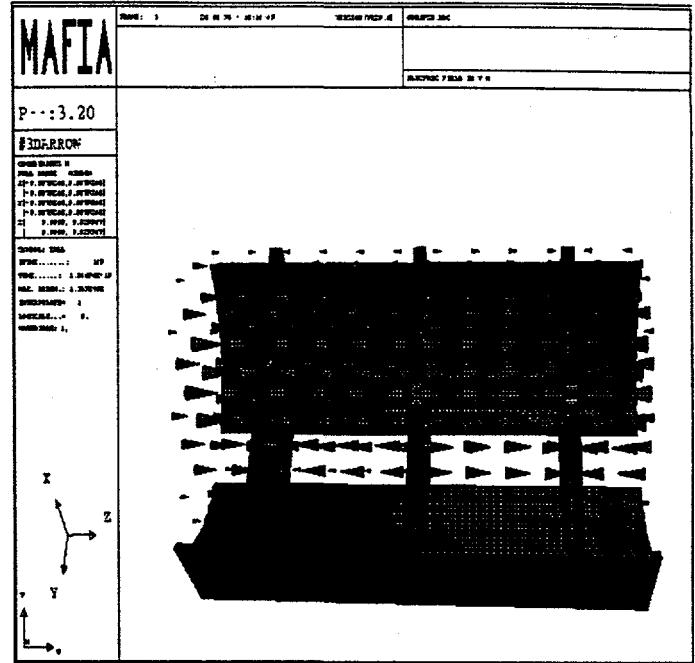generate a standing wave field pattern. An on-axis hole was

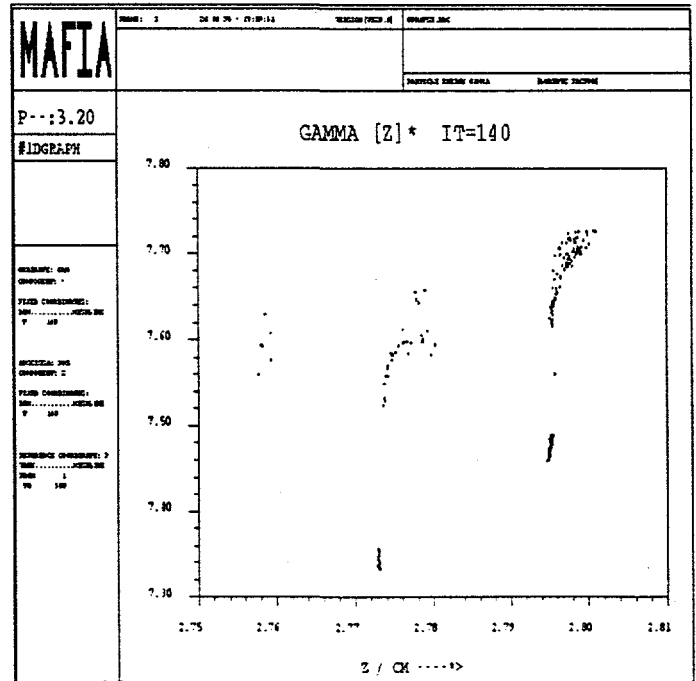Figure 1: Longitudinal field for the accelerated beam

Figure 2: Particle beam energy distribution

drilled in each plate to provide an opening for the bead's travel path. To excite the longitudinal electric field, a field probe of 1.194- mm outer diameter was fabricated. An identical probe was used as a pickup. Two fiber chuck holders held the ends of the fiber line while the bead was pulled through the structure. The bead was advanced through the structure in small

increments (~94 μm/step) through computer control of the stepper motor. At each bead position, the phase of the transmission coefficient, S_{12}, was measured using an HP 8510 network analyzer with an automatic data acuisition system. Figure 4 is the frequency spectrum of the excited modes in the structure.and Figure 5 is a plot of perturbation measurement results of the π–mode.
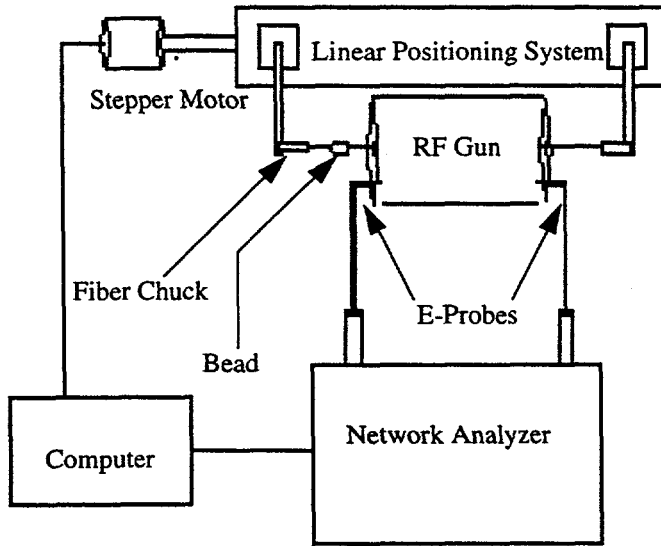

Figure 3: Bead pull field measurement setup

IV. SUMMARY AND DISCUSSION

A 30-GHz photocathode rf gun is being considered as a low emittance electron source for a short-wavelength 50-MeV single pass linac-driven FEL. To understand the rf properties of high-frequency rf gun, a 15-GHz 3 1/2-cell copper structure was fabricated and bench tested. Numerical modeling result using MAFIA give a resonant frequency of 15 GHz for the desired π-mode accelerating field with a shunt impedance of 254MΩ /m (Q=7000). Beadpull measurements of the rf gun resulted in 15.5 GHz for the π-mode with a shunt impedance of 3.4 MΩ/m (Q = 312). The huge discrepancy beween the calculated and measured shunt impedance are mainly due to mechanical imperfections of the cavity during fabrication. This structure was fabricated in many separate pieces with relaxed tolerances and was put together in a "Lego-Block" manner and pressed fitted inside a copper block with a set of bolts and nuts to hold it together at both end. This resulted in poor rf contacts between pieces (cells) which severely affected the rf measurements. Improvements on the structural fabrication and measurement methods are planned.

VI. REFERENCES

[1]   R.L. Sheffield, E.R. Gray and J.S. Fraser,"The Los Alamos Photoinjector Program,"NIM A272 (1988) 222-226

[2]   P. O'Shea, "High Brightness Photo-Cathode Guns for Single Pass X-Ray FELs, 16th International FEL Conference, Stanford, CA, August 21-26, 1994.

[3]   J. Gao, "Theoretical Investigation in the Optimization Design of Microwave Electron Gun," in Proc. 12th Free Electron LAser Conference, 1990.

[4]   K. McDonald, "Design of the Laser-Driven RF Electron Gun for BNL Accelerator Test Facility," IEEE Trans. Electron Devices, vol. 35, no. 11, pp. 2052-2059, 1988.

[5]   K.-J. Kim, Nucl. Instr. and Meth. A 250 (1986) 396.

[6]   R. Klatt, et. al.,"MAFIA, A Three-Dimentional Electromagnetic CAD System," 1986 Linear Accelerator Conference Proc.., SLAC-303,276-278 (1986).

[7]   L. C. Maier and J. C. Slater, "Field Strength Measurements in Resonant Cavities," Journ. Appl. Physics, vol. 23, pp. 68-77, 1952.
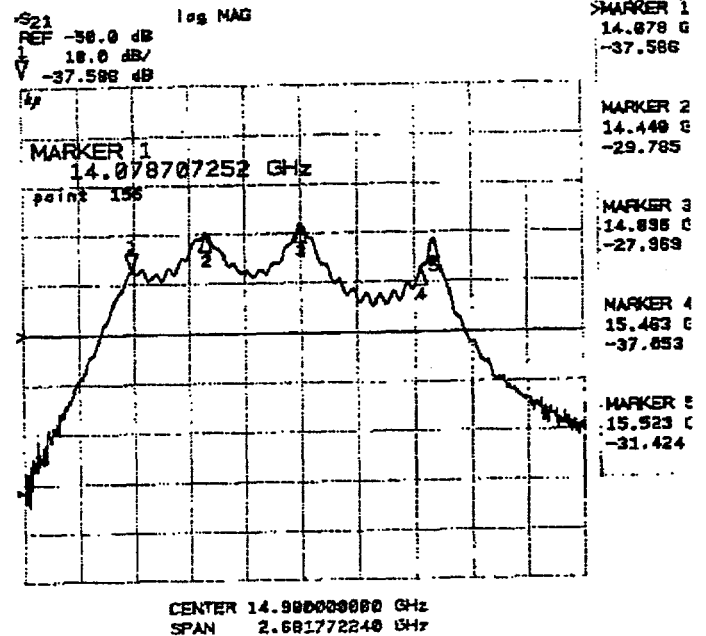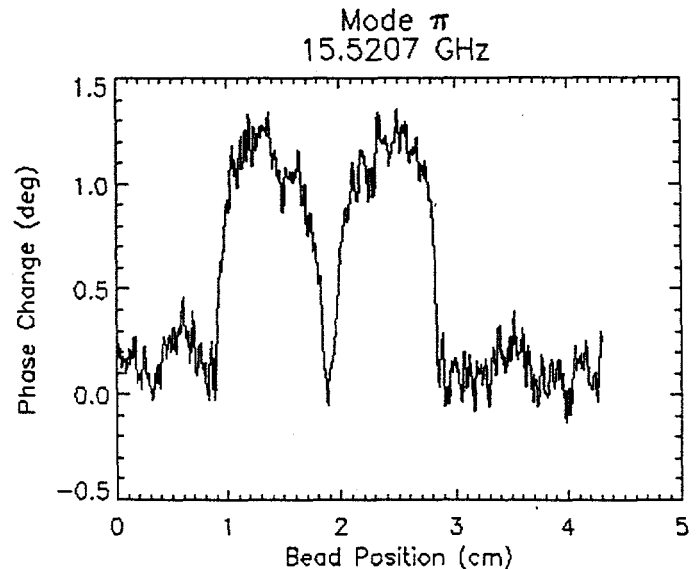
Figure 4: Frequency spectrum of the excited modes

Figure 5: Perturbation measurement result for π-mode